Atomic Structure of Amorphous Metallic $Ni_{81}B_{19}$

P. Lamparter, W. Sperl, and S. Steeb
Max-Planck-Institut für Metallforschung, Institut für Werkstoffwissenschaften, Stuttgart

J. Blétry
St. Gobin Recherche, Aubervilliers, France

Z. Naturforsch. **37a**, 1223—1234 (1982); received July 31, 1982

The three partial Faber Ziman structure factors as well as the Bhatia Thornton structure factors of the metallic glass $Ni_{81}B_{19}$ were evaluated by neutron diffraction experiments using the isotopic substitution method. In one of the investigated specimens the isotopic composition of the components was adjusted in such a way as to make it possible to measure directly with one diffraction experiment the correlation between the metalloid atoms. From the three partial pair correlation functions the atomic distances and the partial coordination numbers are determined. The results demonstrate the strong chemical ordering in amorphous $Ni_{81}B_{19}$. Particularly the distance correlation between the boron atoms turned out to be very pronounced.

The experimental results agree with the main features of a geometrical packing model of soft spheres.

Introduction

For the understanding of the atomic scale structure of binary metallic glasses one needs three partial structure factors and three partial pair correlation functions, respectively. They can be obtained by performing three diffraction experiments with three samples having the same chemical composition, but where the ratio of the scattering factors of both constituent atoms is different. Then the three diffraction experiments yield three total structure factors which provide a system of three independent equations for the evaluation of the three partial structure factors. There are different experimental ways to do this:

Isotopic Substitution Technique

For the performance of this method three samples have to be prepared, where the isotopic abundances and the neutron scattering factors of at least one of both components are different. This technique has been used up to now only for metallic glasses of the metal-metal-type sueh of $Cu_{57}Zr_{43}$ [1,2].

Combination of X-ray and Neutron Diffraction Experiments

This method can be applied in those cases where because of a lack of isotopes the isotopic substitution technique cannot be applied at all or only partly. By this method the partial structure factors of the metallic glass $Fe_{80}B_{20}$ were determined [3]. It has been applied also for Ni-Ti [4] and Cu-Ti [5] glasses.

Magnetic Neutron Scattering Experiments

For magnetic glasses the fact has been used that magnetic atoms have besides their nuclear scattering factor a magnetic scattering factor for neutrons, the magnitude of which can be influenced by the orientation of an external magnetic field and the polarization of the neutrons. With this method the partial structure factors of the metal-metalloid glasses Co-P [6, 7] and Co-B [8] have been determined.

Isomorphous Substitution Technique

One of both components is substituted by another element with similar chemical behaviour but another scattering factor. In [9] the partial structure factors of amorphous Ni-Zr-alloys have been determined with X-ray diffraction substituting Zr by Hf atoms.

Two other ways should be mentioned which however in our opinion nowadays yield no reliable results:

Three Beam Experiment

This method, a combination of neutrons, X-rays, and electrons, fails due to principal difficulties in the quantitative evaluation of the total structure factor from electron diffraction ([10] and [11]).

Reprint requests to Prof. Dr. S. Steeb, Max-Planck-Institut f. Metallforschung, Institut f. Werkstoffwissenschaften, Seestraße 92, D-7000 Stuttgart 1.

0340-4811 / 82 / 1100-1223 $ 01.30/0. — Please order a reprint rather than making your own copy.

Anomalous X-ray Dispersion Method

With this method, different X-ray wavelengths are used in diffraction experiments with the same specimen. This method suffers from the fact that the differences of the scattering factors are so small that even very small experimental uncertainties in the total structure factors lead to large errors in the partial structure factors.

In the present study the isotopic substitution technique has been used to determine the partial structure factors of amorphous $Ni_{81}B_{19}$ by neutron diffraction. A survey of the existing models as well as experimental results for binary metal-metalloid glasses led us to the conclusion that there is nearly no knowledge of the partial pair correlation between the metalloid atoms. On the other hand especially this correlation function should provide a powerful test of theoretical models. Therefore we prepared one of the three samples with a Ni-isotopic mixture which shows a vanishing mean coherent scattering length in order to measure the partial B-B structure factor directly with one diffraction experiment. Preliminary results of the present study have been already reported in [12] and [13].

Fundamentals

In the following a survey of the definitions and equations needed in the present study will be given.

Faber Ziman Formalism

According to the Faber Ziman definition [14] the total structure factor is obtained from the coherently scattered intensity per atom $I_C(Q)$:

$$S^{FZ}(Q) = \frac{I_C(Q) - [\langle b^2\rangle - \langle b\rangle^2]}{\langle b\rangle^2}, \tag{1}$$

where

Q $= 4\pi \sin\theta/\lambda$,

2θ = scattering angle,

λ = wavelength of the radiation,

$\langle b\rangle$ $= c_A b_A + c_B b_B$,

$\langle b^2\rangle$ $= c_A b_A^2 + c_B b_B^2$,

c_A, c_B = atomic concentrations of the components A and B,

b_A, b_B = coherent scattering lengths of A and B.

The total structure factor is a sum of the three weighted partial Faber Ziman structure factors $a_{ij}(Q)$:

$$S^{FZ}(Q) = \frac{c_A^2 b_A^2}{\langle b\rangle^2} a_{AA}(Q) + \frac{c_B^2 b_B^2}{\langle b\rangle^2} a_{BB}(Q) + \frac{2 c_A c_B b_A b_B}{\langle b\rangle^2} a_{AB}(Q). \tag{2}$$

The three partial pair correlation functions $G_{ij}(R)$ are defined as:

$$G_{ij}(R) = 4\pi R\left[\frac{\varrho_{ij}(R)}{c_j} - \varrho_0\right], \tag{3}$$

where

$\varrho_{ij}(R)$ = pair density distribution function of $i-j$ pairs, i.e. number of j atoms per unit volume at distance R from an i atom,

ϱ_0 = mean atomic number density.

The $G_{ij}(R)$ are obtained from the partial structure factors by Fourier transformation from the Q-space to the "real" R-space:

$$G_{ij}(R) = \frac{2}{\pi}\int_0^\infty Q[a_{ij}(Q) - 1]\sin(QR)\,\mathrm{d}Q. \tag{4}$$

In practice the lower and upper integration limits Q_{min} and Q_{max} are given by the 2θ range covered in the diffraction experiment, and the finite integration range leads to so called truncation errors in the calculated correlation functions. The interatomic distances R_{ij} are given by the positions of maxima of the $G_{ij}(R)$ functions.

The partial radial distribution functions $A_{ij}(R)$ can be calculated from the $G_{ij}(R)$:

$$A_{ij}(R) = c_j[4\pi R^2 \varrho_0 + RG_{ij}(R)]. \tag{5}$$

From the $A_{ij}(R)$ functions the partial coordination numbers Z_{ij} can be evaluated:

$$Z_{ij} = \int_{R_l}^{R_u} A_{ij}(R)\,\mathrm{d}R. \tag{6}$$

Hereby the somewhat arbitrary integration limits define an enclosed coordination sphere.

Bhatia Thornton Formalism

Using the Bhatia Thornton formalism [15] the structure of a binary system is described in terms of correlations between density fluctuations and concentration fluctuations, the Fourier transforms of them in Q-space being the partial Bhatia Thorn-

ton structure factors $S_{NN}(Q)$, $S_{CC}(Q)$, and $S_{NC}(Q)$. Here another definition of the total structure factor is convenient:

$$S^{BT}(Q) = \frac{I_C(Q)}{\langle b^2 \rangle} \tag{7}$$

which in terms of the partial structure factors is:

$$S^{BT}(Q) = \frac{\langle b \rangle^2}{\langle b^2 \rangle} S_{NN}(Q) + \frac{c_A c_B (b_A - b_B)^2}{\langle b^2 \rangle} \cdot S_{CC}(Q) + \frac{2\langle b \rangle (b_A - b_B)}{\langle b^2 \rangle} S_{NC}(Q), \tag{8}$$

where

$S_{NN}(Q)$ = partial structure factor of the correlations between number density fluctuations,

$S_{CC}(Q)$ = partial structure factor of the correlations between concentration fluctuations,

$S_{NC}(Q)$ = partial structure factor of the cross correlations between density fluctuations and concentration fluctuations.

For the case of equal partial atomic volumes of the components A and B (no size effect) the structure factor $S_{NC}(Q)$ vanishes. The three density-concentration correlation functions are obtained from the partial structure factors by Fourier transformation from Q-space to R-space:

$$G_{NN}(R) = \frac{2}{\pi} \int Q[S_{NN}(Q) - 1] \sin(QR)\, dQ,$$

$$G_{CC}(R) = \frac{2}{\pi} \int Q[S_{CC}(Q) - 1] \sin(QR)\, dQ, \tag{9}$$

$$G_{NC}(R) = \frac{2}{\pi} \int Q[S_{NC}(Q)] \sin(QR)\, dQ.$$

$G_{NN}(R)$ represents the topological short range ordering (TSRO), whereas $G_{CC}(R)$ represents the chemical short range ordering (CSRO). If the atoms A and B are of different size, G_{NN} and G_{CC} are not independent from each other. The concentration correlation function $G_{CC}(R)$ exhibits maxima at distances between equal atoms and minima at distances between unequal atoms.

Experimental Method

Three amorphous $Ni_{81}B_{19}$ samples were produced as ribbons with a thickness of 13 μm by rapidly quenching the molten alloys on a rotating copper wheel with the melt spinning technique in He atmosphere. The ribbons were cut into small shreds and then pressed into vanadium tubes with 0.1 mm wall thickness, 42 mm height, and 11.5 mm outer diameter.

As boron component the isotope ^{11}B was used (99.2% purity, 97.2% enrichment).

The specimen 1 was prepared using nickel with natural isotopic composition, ^{nat}Ni. The specimen 3 was prepared using the isotope ^{62}Ni (98.5% enriched). The specimen 2 contained a mixture of 26.6 at.% ^{62}Ni (99% enriched) and 73.4 at.% ^{60}Ni (95.4% enriched), a mixture for which the negative scattering length of ^{62}Ni ($-0.852 \cdot 10^{-12}$ cm) and the positive scattering length of ^{60}Ni ($0.309 \cdot 10^{-12}$ cm) yield a resultant zero coherent scattering length. This mixture will be called $^{\varnothing}Ni$ in the following.

The neutron diffraction experiments were performed with the D2 diffractometer at the high flux reactor of the Institute Laue Langevin, Grenoble (see [16]). To cover a Q-range as extended as possible, two different wavelengths, $\lambda_1 = 1.22$ Å and $\lambda_2 = 0.824$ Å, were applied.

The diffraction patterns were recorded within the range of the scattering angle $1.4° < 2\theta < 120°$ with λ_1 and $38° < 2\theta < 120°$ with λ_2. The angular distance of the measured points with the 64-cell multicounter was $\Delta 2\theta = 0.2°$. For the necessary corrections for background scattering and for scattering and absorption of the vanadium container, additional scans were made with empty instrument, with empty container, and with a cadmium rod which had the same dimensions as the samples. The minimum collected number of counts per measured point was $1.5 \cdot 10^5$ for specimens 1 and 2, and $0.6 \cdot 10^5$ for specimen 3.

In order to determine the absorption cross sections σ^a of the used Ni-materials and the boron the total cross sections σ^t of ^{nat}Ni, ^{62}Ni, $^{\varnothing}Ni$, and ^{11}B were measured by a transmission experiment, using $\lambda = 1.03$ Å, with flat specimens before alloying the nickel and the boron. σ^a was then obtained by subtracting the coherent cross section and the incoherent cross section from σ^t. The values for the other wavelengths listed in Table 1 were calculated according to

$$\sigma^a(\lambda) = \sigma^a(\lambda = 1.03)\, \lambda / 1.03. \tag{10}$$

The macroscopic density D of amorphous $Ni_{81}B_{19}$

with natural Ni was measured by the Archimedean method using Dibromoethane as fluid. We obtained $D = 8.4$ g/cm³. From this value also the densities of the glasses with ^{62}Ni and $^{\varnothing}$Ni could be calculated.

Data Reduction

In Figs. 1 and 2 the measured diffraction patterns are shown. They were corrected for background scattering, for container scattering and for absorption in the container and in the sample according to Paalmann and Pings [17]. The normalization of the corrected intensity data was done with the Krogh Moe method [18]. Hereby the incoherent scattering and the multiple scattering contributions are subtracted, the latter being calculated corresponding to [19]. This yielded the coherently scattered intensity per atom $I_C(Q)$, from which the total structure factor is obtained using (1) or (7).

The absorption- and scattering parameters used for the data reduction are listed in Table 1. The coherent scattering lengths of the isotopically enriched Ni-materials were calculated from tabulated values for the pure Ni-isotopes [20], taking the isotopic abundances of the isotopes $^{58, 60, 61, 62, 64}$Ni within these materials into account.

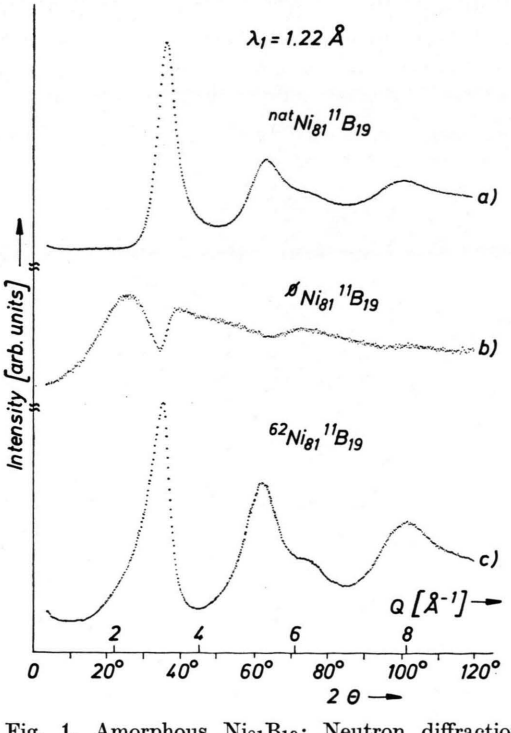

Fig. 1. Amorphous $Ni_{81}B_{19}$; Neutron diffraction ($\lambda = 1.22$ Å); Experimental intensities.

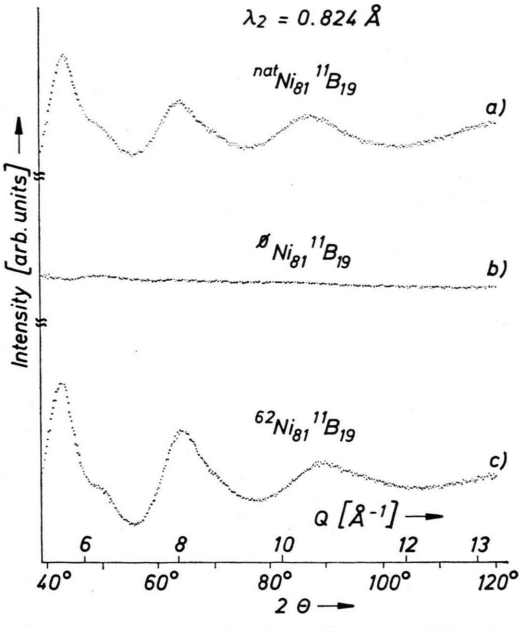

Fig. 2. Amorphous $Ni_{81}B_{19}$; Neutron diffraction ($\lambda = 0.824$ Å); Experimental intensities.

The incoherent cross sections σ^{inc} of the enriched ^{62}Ni- and of the $^{\varnothing}$Ni-material were calculated from the expression for the isotopic incoherence

$$\sigma^{inc} = 4\pi\left[\sum_K x_K b_K^2 - \left(\sum_K x_K b_K\right)^2\right], \qquad (11)$$

where x_K = concentration of the isotope ^{K}Ni in the enriched material and $K = 58, 60, 61, 62, 64$. The spin incoherence of ^{61}Ni, which is the only one having a nuclear spin, was neglected because of the very small concentration of this isotope. The values finally obtained are listed in Table 1.

Table 1. Absorption- and scattering-parameters: σ^a = absorption cross section, σ^{inc} = incoherent scattering cross section, b = coherent scattering length, * for the explanation of this slightly positive value see text.

Component	σ^a [barn] $\lambda = 1.22$ Å	b [10^{-12} cm]	σ^{inc} [barn]
^{11}B (97.2% enr.)	17.24	0.6 [20]	0.6 [3]
^{nat}Ni	3.25	1.03 [20]	4.8 [21]
^{60}Ni (pure)	—	0.28 [20]	0 [22]
^{60}Ni (95.4% enr.)	—	0.309	0.53
^{62}Ni (pure)	—	−0.87 [20]	0 [22]
^{62}Ni (98.5% enr.)	9.82	−0.844	0.61
$^{\varnothing}$Ni (0.734 ^{60}Ni + 0.266 ^{62}Ni)	3.20	0.03*	3.9

The intensity curves in Figs. 1 and 2 do not oscillate around a horizontal line, as they should if the scattering were purely elastic, but around a line which lowers at higher Q values. This behaviour is caused by inelastic neutron scattering, and it is most pronounced for the specimen 2 with $^{\varnothing}$Ni. The comparison of Fig. 1 with Fig. 2 shows that the influence of inelastic scattering is increasing with increasing wavelength λ of the neutrons. The usual correction method for inelastic scattering according to Placzek [23], which is often applied successfully in the case of liquid specimens where the atoms can move more or less freely, turned out to fail completely for the $^{\varnothing}$Ni-specimen. Due to the lack of inelastic scattering experiments with metallic glasses up to now there exist to our knowledge no theoretical correction methods for inelastic scattering effects. Therefore the correction had to be done in a somewhat arbitrary way, which was carried out after the background- and absorption corrections: The intensities were multiplied by a function $F(Q)$ which is increasing with Q. Thereby a linear as well as a quadratic Q-dependence of $F(Q)$ was tested. The criterion for the best choice of $F(Q)$ was the visual observation whether the corrected curve oscillates properly around a horizontal line or not. The linear function $F(Q)=1+CQ$ turned out to give the most reasonable results, where the constant C depended on the specimen no. and on λ. Possible errors caused by the choice of $F(Q)$ are expected to cause long-wavelength-errors in the structure factors and therefore unphysical oscillations in the Fourier transforms at small R values. It should be mentioned that the corrections for the specimen 1 and 3 had to be only very small as can be seen in Figs. 1 and 2.

Before performing the normalization procedure, the two curves for each specimen, plotted versus Q, were combined to one curve by fitting the λ_2-curve on the λ_1-curve in the region of overlap.

The normalization of the corrected intensity curve of specimen 2 yielded at small Q values a negative value of $S_2^{BT}(Q)$. Whether this unphysical behaviour resulted from incorrect data for the incoherent scattering or from the correction procedure for inelastic scattering described above is not clear. Therefore the curve had to be renormalized by adding a constant which was chosen such that $S_2^{BT}(Q)$ equals zero at small Q values. This clearly is the minimum procedure which must be done since per definition $S^{BT}(Q)$ can not become negative. This correction affected to some extend the partial structure factor $a_{BB}(Q)$ and the partial Bhatia Thornton structure factors at low Q's, but had only small influence at higher Q's and nearly no influence on $a_{NiNi}(Q)$ and $a_{NiB}(Q)$. In [13] this correction had not been done, which explains the slight differences between those preliminary results and the present work.

Results

Total and Partial Structure Factors

Figure 3 shows the total structure factors $S_1(Q)$, $S_2(Q)$ and $S_3(Q)$ finally obtained for specimens 1, 2 and 3. With the scattering lengths from Table 1 the total Faber Ziman structure factors (2) become

$$\begin{aligned} S_1^{FZ}(Q) &= 0.774\,a_{NiNi}(Q) + 0.015\,a_{BB}(Q) \\ &\quad + 0.212\,a_{NiB}(Q), \\ S_2^{FZ}(Q) &= 0.031\,a_{NiNi}(Q) + 0.680\,a_{BB}(Q) \\ &\quad + 0.290\,a_{NiB}(Q), \\ S_3^{FZ}(Q) &= 1.440\,a_{NiNi}(Q) + 0.040\,a_{BB}(Q) \\ &\quad - 0.480\,a_{NiB}(Q). \end{aligned} \tag{12}$$

From the large differences between the corresponding coefficients it is readily seen that the three par-

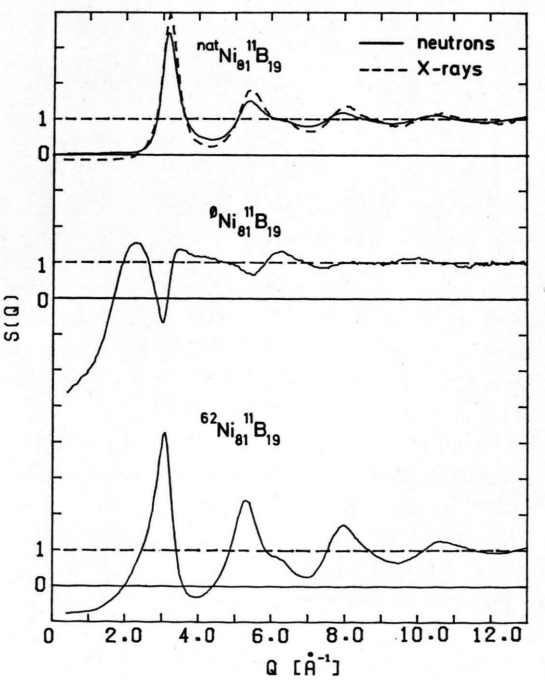

Fig. 3. Amorphous $Ni_{81}B_{19}$; Total Faber Ziman structure factors.

tials are very well defined by this set. The value of the normalized coefficient determinant (see [3]) is 0.5, which is half of the optimum value 1.

At this point a remark concerning the coherent scattering length of the so called $^{\varnothing}$Ni must be made: When b ($^{\varnothing}$Ni) was taken as zero, as intended in preparing this material, it turned out during the calculation of the partial structure factors and the partial correlation functions that $a_{BB}(Q)$ as well as $G_{BB}(R)$ showed a small peak at that positions where the functions $a_{NiB}(Q)$ and $G_{NiB}(R)$ have their first maximum. From this observation we concluded that $S_2^{FZ}(Q)$ is influenced to some extent by the Ni-B correlation, that means that the condition $b(^{\varnothing}\text{Ni})=0$ was not ideally met during the preparation of this material. For the determination of the residual scattering length of $^{\varnothing}$Ni we repeated the calculation of the partial functions using varying $b(^{\varnothing}\text{Ni})$-values in such a way that finally $a_{BB}(Q)$ and $G_{BB}(R)$ showed no longer a contribution from Ni-B correlations. This method finally lead to $b(^{\varnothing}\text{Ni}) = 0.03 \cdot 10^{-12}$ cm. It should be noted that even this very small value causes a remarkable weight-factor of the $a_{NiB}(Q)$ function in equation (12) for the total structure factor $S_2^{FZ}(Q)$.

The total Bhatia Thornton structure factors (8) become

$$\begin{aligned} S_1^{BT}(Q) &= 0.969\, S_{NN}(Q) \\ &\quad + 0.031\, S_{CC}(Q) + 0.879\, S_{NC}(Q), \\ S_2^{BT}(Q) &= 0.277\, S_{NN}(Q) \\ &\quad + 0.723\, S_{CC}(Q) - 2.281\, S_{NC}(Q), \\ S_3^{BT}(Q) &= 0.503\, S_{NN}(Q) \\ &\quad + 0.497\, S_{CC}(Q) - 2.549\, S_{NC}(Q). \end{aligned} \tag{13}$$

The value of the normalized coefficient determinant for the three equations (13) is 0.3. Figure 4 shows the partial Faber Ziman structure factors calculated from (12) and Fig. 5 the partial Bhatia Thornton structure factors calculated from (13).

The pronounced oscillations of the concentration-concentration structure factor $S_{CC}(Q)$ around unity indicate already strong chemical ordering in the $Ni_{81}B_{19}$ glass. The oscillations of $S_{NC}(Q)$ around zero show a marked size effect in the atomic structure. The ratio of the first peak positions of S_{CC} and S_{NN} in Q equals 0.82, which is in contrast with the corresponding value of about 0.6 found in metal-metal glasses such as Cu-Ti [5] and liquid metallic substitutional alloys with compound forming tendency. This observation again reflects a marked size effect and proves that amorphous Ni-B is not a substitutional alloy.

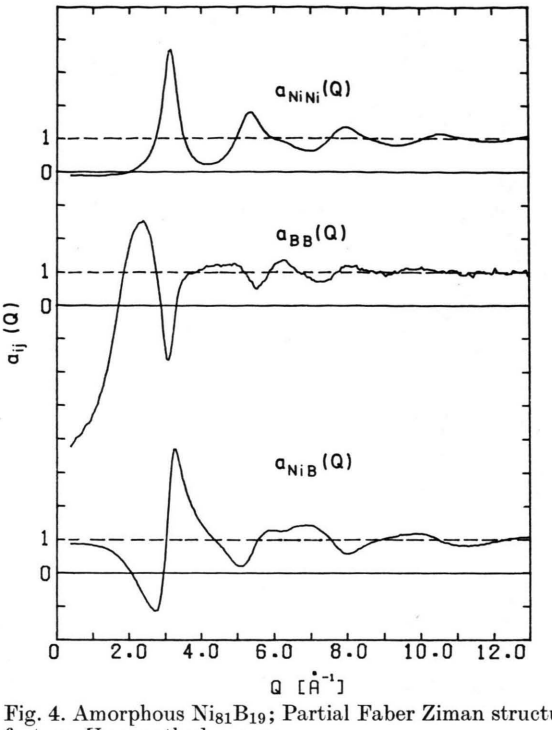

Fig. 4. Amorphous $Ni_{81}B_{19}$; Partial Faber Ziman structure factors. Unsmoothed curves.

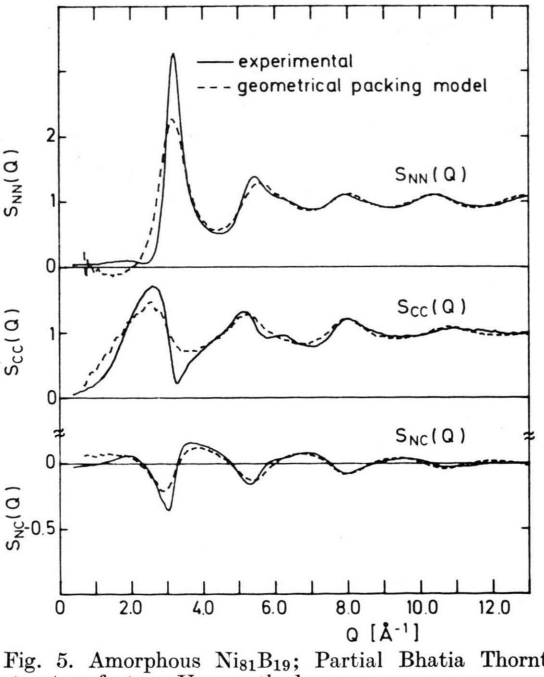

Fig. 5. Amorphous $Ni_{81}B_{19}$; Partial Bhatia Thornton-structure factors. Unsmoothed curves.

Correlation Length

From the half-width $\Delta Q^{I}_{CC} = 1.36\,\text{Å}^{-1}$ of the main peak of $S_{CC}(Q)$ one can calculate acccording to the Scherrer-formula $\xi_{CC} = (2\pi/\Delta Q^{I}_{CC})$ the correlation length $\xi_{CC} \cong 5$ Å (of the concentration fluctuations i.e. of the chemical short range order. The corresponding correlation length $\xi_{NN} = 11$ Å is accordingly obtained by $\xi_{NN} = (2\pi/\Delta Q^{I}_{NN})$ from the half with $\Delta Q^{I}_{NN} = 0.55\,\text{Å}^{-1}$ of the main peak of $S_{NN}(Q)$.

This means that the range of correlation between the concentration fluctuations (Chemical short range order = CSRO) is clearly smaller than that between the density fluctuations (Topological short range order = TSRO).

Atomic Correlation Functions

Figure 6 shows the three partial pair correlation functions $G_{ij}(R)$ calculated from the partial Faber Ziman structure factors using (4). The boron-boron correlation function exhibits very interesting features: It's main maximum shows a double peak structure, from which we learn that there exist two different well defined B-B distances in the metallic glass. Furthermore we notice, regarding the oscillations of the $G_{ij}(R)$ functions, that the range of correlation between the boron atoms is as extended as that between the Ni-Ni- and the Ni-B-pairs.

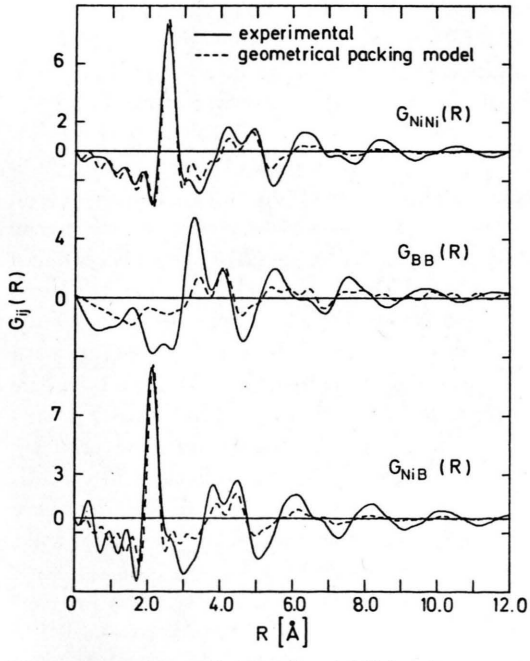

Fig. 6. Amorphous $Ni_{81}B_{19}$; Partial Faber Ziman pair correlation functions. For the calculation of the G_{BB} curve the a_{BB} curve in Fig. 4 was smoothed by a cubic splinefit.

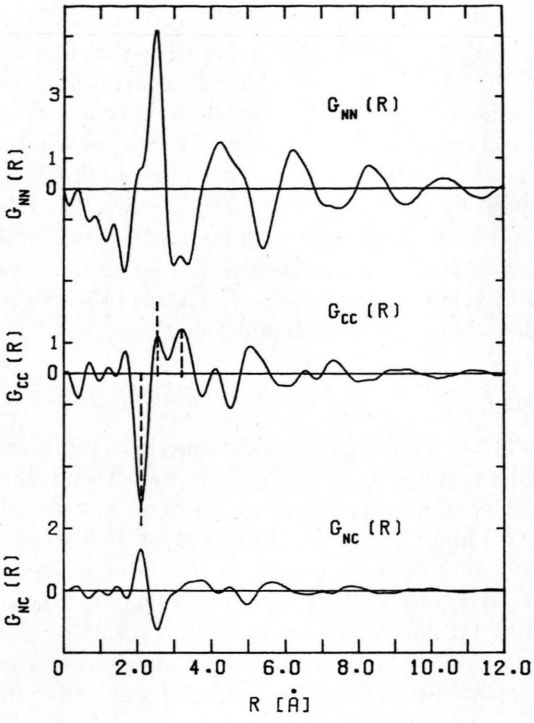

Fig. 7. Amorphous $Ni_{81}B_{19}$; Partial Bhatia Thornton density-concentration correlation functions.

Concerning the peak positions of the three correlation functions we make an interesting observation: When we shift the G_{BB} function by $\Delta R = 0.9$ Å and the G_{NiB} function by $\Delta R = 0.425$ Å to the right hand side, the positions of the maxima and minima of the three curves coincide with the exception that the G_{BB} curve has no maximum at that position where the G_{NiNi} curve and the G_{NiB} curve show their first main peak. This coincidence is to be explained by strong chemical ordering of the Ni- and the B-atoms because on the other hand statistical distribution of two kinds of atoms in a binary alloy would rather result in a scaling of the R values with the atomic diameters than in a shift.

From the partial Bhatia Thornton structure factors the three density-concentration correlation functions G_{NN}, G_{CC}, and G_{NC} were calculated, using (9), and plotted in Figure 7. The density-density correlation function $G_{NN}(R)$ represents the topological ordering. The main peak shows the contribution

of nearest Ni-Ni neighbours at it's maximum and the contribution of Ni-B neighbours as a shoulder at a smaller atomic distance. The concentration-concentration correlation function shows up the strong chemical ordering in amorphous $Ni_{81}B_{19}$, as can be seen from the pronounced negative first peak which is caused by the unlike Ni-B atomic pairs. The following two positive peaks can be ascribed to Ni-Ni pairs and B-B pairs, respectively, and so on. The cross correlation function $G_{NC}(R)$ again reflects the considerable size effect already mentioned.

Atomic Distances and Partial Coordination Numbers

From the $G_{ij}(R)$ correlation functions the individual atomic distances R_{ij} were taken and the partial coordination numbers Z_{ij} were calculated using (5) and (6). The results are given in Table 2. The distance between nearest Ni neighbours $R_{NiNi} = 2.52$ Å agrees well with the Goldschmidt diameter of Ni (2.48 Å according to [24]). Presuming the diameter of the Ni-atom to be independent of the kind of it's neighbours the diameter of the boron atoms can be calculated according to (14):

$$d_B = 2\,R_{NiB} - R_{NiNi} = 1.70\ \text{Å}. \qquad (14)$$

The value $d_B = 1.70$ Å is in good accordance with the value of 1.72 Å found for the case of $Fe_{80}B_{20}$ [3] as well as with 1.76 Å given in [25] as diameter of fourfold coordinated covalently bound boron atoms.

In the following some illustrations of experimental coordination numbers will be given: Comparing experimentally derived coordination numbers with models for amorphous structures one must keep in mind that the former are not unequivocal, but that there are several ways to extract them from experimental $A(R)$-curves. The values given in Table 2 are obtained with the minimum-minimum method, that means the $A_{ij}(R)$ curves were integrated between the minimum at R_l preceding and the minimum at R_u following the peak of a certain coordination sphere. The values for R_l and R_u are also given in Table 2. Figure 6 shows, however, that the $G_{NiNi}(R)$- as well as the $G_{NiB}(R)$-curve have a small bump or a shoulder, respectively, on the right hand side of their main peak. The question arises now whether this feature, which can be observed with many experimental $G(R)$-functions found in the literature, is an artefact due to the Fourier transformation within the limited Q-range covered by the experiment, or whether it reflects really additional atoms located in the first coordination sphere at somewhat greater distances. In the latter case the pair correlations would be asymmetric with respect to the mean distance. In Fig. 8 we propose a method how to obtain a quantitative description of this asymmetric behaviour, illustrated for the case of $G_{NiB}(R)$. The experimental $G_{NiB}(R)$ is again plotted as solid line. This curve was fitted by a sum

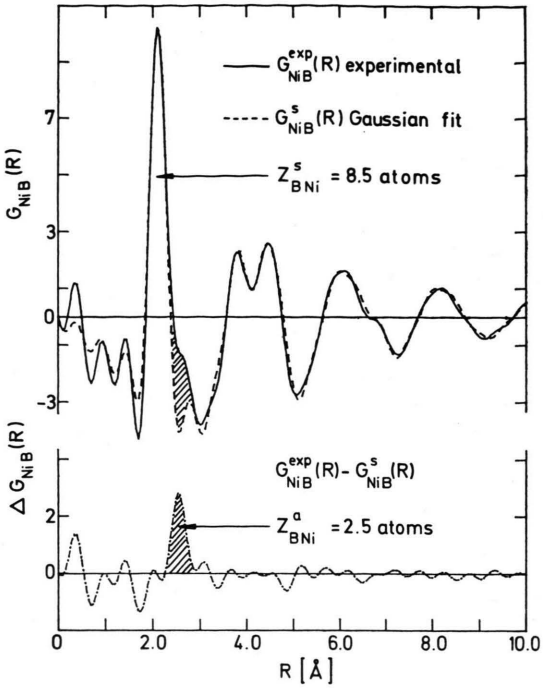

Fig. 8. Amorphous $Ni_{81}B_{19}$; Determination of the symmetric coordination number Z^s_{BN} from G_{NiB}.

Table 2. Structural properties of amorphous $Ni_{81}B_{19}$: R_{ij} = atomic distance; Z_{ij} = partial coordination number (j atoms around a central i atom); σ_1 = width of the first coordination sphere; R_l, R_u = lower and upper integration limits for the calculation of Z_{ij}; Q_{max} = maximum Q value for the Fourier transformation of the structure factor.

Atomic pair $i-j$	R_{ij} [Å]	Z_{ij}	σ_1 [Å]	R_l [Å]	R_u [Å]	Q_{max} [Å^{-1}]
Ni-Ni	2.52	10.8	0.34	2.15	3.00	12.53
B-Ni	2.11	9.3	0.32	1.80	2.55	12.26
Ni-B	2.11	2.2		1.80	2.55	12.26
B-B	3.29	3.6		2.65	3.70	9.35
	4.02	3.7		3.70	4.60	

of Gaussian curves, plotted as dashed curve $G^{s}_{NiB}(R)$

$$G^{s}(R) = -4\pi\varrho_0 R + \sum_{m=1}^{10} \frac{Z_m}{\sqrt{2\pi}\,\varepsilon_m R_m} \cdot \left[\exp\left(-\frac{(R-R_m)^2}{2\varepsilon_m^2}\right) - \exp\left(-\frac{(R+R_m)^2}{2\varepsilon_m^2}\right)\right], \quad (15)$$

where R_m = position, $\sigma_m \cong 2.335\,\varepsilon_m$ = width, and $Z_m = Z_{ij}/c_j$ = area of the Gauß curve m are three parameters for fitting of the coordination sphere m (the second exponential term is negligible for $R > 0$ and was introduced for mathematical reasons).

As stressed above the ghost ripples introduced by the truncation error during the Fourier transformation are important in the neighbourhood of the main peak of $G(R)$. Therefore the model curve had to be modified artificially by a corresponding termination error before comparing it to the experimental curve. This was done by transforming $G^{s}(R)$ into Q-space, cutting it at the maximum experimental Q-value Q_{max}, and then transforming it back into R-space.

By the fit of the model curve $G^{s}(R)$ to the experimental curve $G^{exp}(R)$ a so called symmetric coordination number Z^{s}_{ij} is defined from the area of the first Gauß curve Z_1, and we obtained for the case of the Ni-B correlation:

$$Z^{s}_{BNi} = 8.5\,.$$

This value is smaller than the value 9.3 in Table 2 obtained with the minimum-minimum method.

Comparison of the curves in Fig. 8 shows that the level of the experimental curve at the right hand side of the main maximum is higher than that of the model curve, this fact being not caused by termination errors but by an asymmetric contribution of the experimental $G_{NiB}(R)$ function (hatched area). The difference curve

$$\Delta G_{NiB}(R) = G^{exp}_{NiB}(R) - G^{s}_{NiB}(R)$$

exhibits a maximum at $R = 2.5$ Å, the area of its corresponding $A(R)$ function giving the asymmetric contribution Z^{a}_{BNi} to the coordination number Z_{BNi}:

$$Z^{a}_{BNi} = 2.5\,.$$

Finally we define a so called asymmetric coordination parameter

$$n = Z^{a}/(Z^{a} + Z^{s}), \quad (16)$$

and we obtain $n_{BNi} = 0.23$.

We note that the asymmetric behaviour of the pair correlation functions in metallic glasses plays an important role in the evaluation of the data from EXAFS experiments as discussed for example in [26], and that general regularities are expected to be gained from the treatment of already existing $G(R)$-functions and of those which will be measured in the future with the method proposed above.

The widths σ_1 of the first Gaussian peak of $G^{s}(R)$ are included in Table 2 for the Ni-Ni- and the Ni-B-correlation. They are smaller than the corresponding widths of the first peaks of the experimental $G_{NiNi}(R)$ and $G_{NiB}(\cong 0.4$ Å), the latter being broadened by the truncation effect. Interestingly the values of σ_1 are nearly equal whereas for the case of the $Fe_{80}B_{20}$ glass [3] the metal-metalloid correlation was found to be sharper than the metal-metal correlation. This observation indicates different chemical interaction between Fe and B and between Ni and B as was supposed already from the results of [27].

Short Range Order Parameter η_{NiB}

Alternatively to the Warren-Cowley short range order parameter [28] which applies for substitutional binary alloys, Cargill and Spaepen [29] have defined a short range order parameter for non substitutional alloys, where the coordination numbers of the two kinds of atoms are different. The calculation was done from the partial coordination numbers $Z_{NiNi} = 10.8$ and $Z_{NiB} = Z_{BNi}c_B/c_{Ni} = 2.2$ in the same way as shown in [3] for the case of glassy $Fe_{80}B_{20}$, and we obtained:

$\eta_{NiB} = 0.17$, which corresponds to the maximum possible value.

Geometrical Packing Model of Soft Spheres for Binary Alloys

In [30] and [31] geometrical models for the structure of binary metallic alloys have been built up by constructing assemblies of 5000 hard spheres with two different sizes. In the unsymmetrical packing algorithm, in order to take into account the preferred chemical interaction between different atoms in a metal-metalloid glass, the aggregate was grown with the ordering rule that small spheres were forbidden to be in hard contact. The softness of all spheres was then simulated by introducing oscillations of the atoms with a certain frequency at a

given temperature. This led to a certain mean square deviation of the atoms from their equilibrium positions, i.e., a broadening of first neighbour peaks of the pair correlation functions.

We used this model for the case of 20 at.% small spheres and a sphere diameter ratio 1.45. This value is close to 1.48, which is obtained from the atomic diameters of Ni (2.52 Å) and of B (1.70 Å). The diameter of the small spheres was chosen as 1.74 Å in order to make the diameter of the large spheres equal to that of the Ni atoms. The vibrational frequency was taken as $5 \cdot 10^{12}\ s^{-1}$ and the temperature as 295 K.

The atomic density of the model cluster came out as $\varrho_0 = 0.074\ Å^{-3}$, which is clearly smaller than that of the $Ni_{81}B_{19}$ glass ($0.102\ Å^{-3}$). Therefore the density of the cluster was adjusted to the real density by scaling the amplitudes of the structure factor oscillations with 0.102/0.074.

From the positions of the 5000 atoms the partial pair density distribution functions $P_{ij}(R)$ were calculated, which are defined as

$$P_{ij}(R) = \varrho_{ij}(R)/(c_j \varrho_0)\,. \tag{17}$$

Figure 9 shows the results.

From the $P_{ij}(R)$ functions the partial Faber Ziman structure factors $a_{ij}(Q)$ as well as the partial Bhatia Thornton structure factors $S_{kl}(Q)$ were obtained by Fourier transformation. For comparison the three partial Bhatia Thornton structure factors are plotted in Fig. 5 as dashed curves together with the experimental ones of $Ni_{81}B_{19}$ as solid curves.

It can be seen that the general features are well described by the geometrical model: The maxima and minima positions of all the three partials are in accordance. The $S_{CC}(Q)$ function shows that the chemical short range order is described in principal by the simple rule that the metalloid atoms do not touch each other. As can be seen, however, from the sharp minimum following the first maximum and from the double peak structure at the second maximum the experimental $S_{CC}(Q)$ function exhibits more detailed structure than the model curve. This indicates that the chemical ordering is more pronounced and more extended in the real glass than in the model cluster. The $S_{NC}(Q)$ curve shows that also the size effect is represented by the model in a very good way.

For comparison of the partial correlation functions not the $P_{ij}(R)$ curves of Fig. 9 were taken,

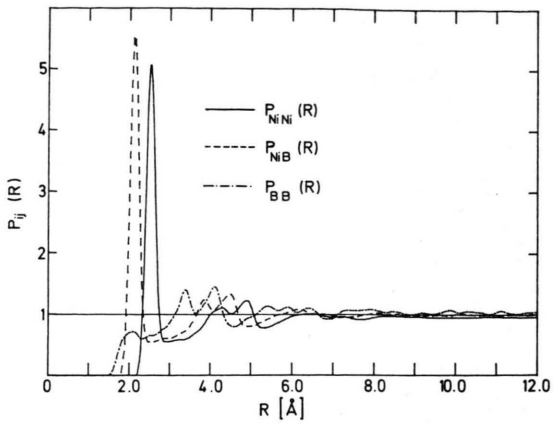

Fig. 9. Geometrical packing model for amorphous $Ni_{81}B_{19}$; Partial pair distribution functions $P_{ij}(R)$.

but the partial $G_{ij}(R)$ curves which were obtained by Fourier transformation of the model partial Faber Ziman structure factors. Hereby the same integration limits Q_{max} as for the experimental curves were taken in order to simulate the same termination effects. Figure 6 shows the model curves as dashed lines together with the experimental curves.

The positions of the peaks, i.e. the atomic distances are described exactly by the geometrical model. The damping of the oscillations, however, goes faster in the model curves than in the experimental ones from which we note again that the range of ordering is more extended in the real Ni-B glass. The splitting up of the second maximum of the $G_{NiNi}(R)$- and of the $G_{NiB}(R)$-function is reproduced by the model. Furthermore the double peak structure of the boron-boron correlation, which is in our opinion a very important result of the present experimental study, is shown also in the model $G_{BB}(R)$ curve. From the discrepancy of the relative amplitudes of the two subpeaks we conclude that there exists more detailed chemical interaction in the real glass than just the avoidance of nearest metalloid neighbours. The model $G_{BB}(R)$ curve exhibits a small maximum at 2.1 Å (compare also Fig. 9) which is larger than the hard contact distance between small spheres and therefore not forbidden in the model. Unfortunately a comparison with the experimental $G_{BB}(R)$ curve is not possible in this low R-region because the problems during the data reduction for specimen 2 led to uncertainties at small distances as explained before.

As resumé we note that the geometrical model describes fairly well the general features of the $Ni_{81}B_{19}$ glass and that improvements of the details are expected from relaxation calculations with the model cluster.

Other Models

In dense random packing models of hard or soft spheres the molecular units for the construction of a model cluster are single atoms and chemical ordering effects are simulated by specific rules incorporated in the packing algorithms. There exist, however, alternative approaches for modelling amorphous structures where the structural units are clusters which have already a distinct chemical order.

Quasicrystalline Models

In the quasicrystalline models the short range order is supposed to be close to that in corresponding crystalline phases. Ni and B form orthorhombic crystalline Ni_3B with two Ni sites with different coordination, one having two and one having three nearest B neighbours [32]. The mean Ni-Ni coordination number Z_{NiNi} equals 11.3, and the B-Ni coordination number is $Z_{BNi}=6$. These values differ clearly from the corresponding figures in Table 2 for the $Ni_{81}B_{19}$ glass. In previous studies a fair correspondence of the chemical short range order in the glasses and related crystalline phases was stated for the case of Fe-B- and Co-B glasses ([3], [13]). In the light of the results of the present work, however, we must note that this question needs further investigation.

Model Built From Coordination Polyhedron with Defined Local Geometry

In Ref. [33] a packing model was proposed where the polyhedra are trigonal prisms formed by six metallic neighbours around a central metalloid atom. Three further metal atoms are capping the square faces of the prism at a somewhat larger distance from the central atom. In Fig. 10 it is shown how the packing of the next prism follows on the base of the triangle formed by two atoms of the first prism and one cusp-atom. If we take as distance of the six metal atoms from the center the value $R_{NiB}=2.11$ Å from Table 2, the nearest possible distance of the three cusp-atoms from the center equals 2.29 Å. That means that the first

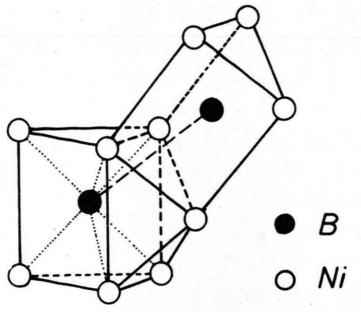

Fig. 10. Trigonal prismatic packing model: The cusp-atom of one of three square faces is shown which forms together with two edge sharing atoms the triangular base for another trigonal prism.

maximum of the pair correlation function $G_{BNi}(R)$ representing the first nine Ni neighbours of a B atom would show an asymmetric behaviour. This is not observed at the main peak of $G_{BNi}(R)$ in Fig. 8, where the distribution of 8.5 Ni neighbours could be described by a Gaussian curve. Close contact of the three cusp-atoms to the central metalloid atom, i.e. symmetrical distance distribution of the nine metallic neighbours would require a larger diameter of the metalloid atom (1.85 Å).

The packing of two trigonal prisms as shown in Fig. 10 yields 3.13 Å as distance between their centers. This distance should represent the nearest B-B distance. Comparison with the figures in Table 2 shows that the B-B distances are larger in the Ni-B glass (3.29 Å and 4.02 Å).

Conclusions

The partial structure factors and the partial pair correlation functions of the metallic glass $Ni_{81}B_{19}$ have been obtained with neutron scattering experiments using the isotopic substitution technique. The main intention has been the direct experimental observation of the distribution of the metalloid atoms in the amorphous metal-metalloid structure, because especially from the knowledge of this distribution a powerful tool for the construction of structural models was expected. The boron-boron correlation function proves that the distribution of the metalloid atoms is by no means statistical: There exist two different well defined distances between "nearest" boron neighbours, and the extension of the correlation range is as large as for Ni-Ni- and Ni-B-atomic pairs. Due to experimental difficulties

the existence of rarely occuring direct B-B contact could not be excluded definitely.

The partial coordination numbers as well as the features of the partial Bhatia Thornton structure factors show that the structure of the $Ni_{81}B_{19}$ glass is governed strongly by chemical ordering between the Ni atoms and the B atoms.

A geometrical packing model with soft spheres has been applied for the simulation of the structure of $Ni_{81}B_{19}$. It could be shown that the general features of the atomic distribution functions, especially the double peak structure of the B-B correlation function, can be represented by the model when direct contact between the metalloid atoms is prohibited.

The results of the present work show that the clarification of the question whether the local chemical ordering in metallic glasses resembles the structure of related crystalline phases or not needs further investigation.

Acknowledgements

Thanks are due to the Deutsche Forschungsgemeinschaft, Bad Godesberg, and to the Verein Deutscher Gießereifachleute, Düsseldorf, for financial support. Thanks are also due to Kernforschungszentrum, Karlsruhe, for allocation of beam time and to the Laue-Langevin Institute, Grenoble, for granting measuring time at the high flux reactor.

[1] T. Mizoguchi, T. Kudo, T. Irisawa, N. Watanabe, N. Niimura, M. Misawa, and K. Suzuki, Proc. 3rd Int. Conf. Rapidly Quenched Metals, Brighton **2**, 384 (1978).
[2] P. Lamparter, G. Rainer-Harbach, and S. Steeb, Annex to the Annual Report, Inst. Laue Langevin, Grenoble 1980, p. 261.
[3] E. Nold, P. Lamparter, H. Olbrich, G. Rainer-Harbach, and S. Steeb, Z. Naturforsch. **36a**, 1032 (1981).
[4] H. Ruppersberg, D. Lee, and C. N. J. Wagner, J. Phys. F: Metal Phys. **10**, 1645 (1980).
[5] M. Sakata, N. Cowlam, and H. A. Davies, J. de Physique C8, **41**, 190 (1980).
[6] J. Blétry and J. F. Sadoc, Phys. Rev. Letters **33**, 172 (1974).
[7] J. Blétry and J. F. Sadoc, J. Phys. F: Metal Phys. **5**, L 110 (1975).
[8] J. M. Dubois, P. Chieux, G. Le Caer, J. Schweitzer, and J. Blétry, Proceedings of the Montpellier Conference from July 1982. (1983) in press.
[9] C. N. J. Wagner and D. Lee, J. de Physique C8, **41**, 242 (1980).
[10] F. Paasche, H. Olbrich, U. Schestag, P. Lamparter, and S. Steeb, Z. Naturforsch. **37a**, 1139 (1982).
[11] F. Paasche, H. Olbrich, G. Rainer-Harbach, P. Lamparter, and S. Steeb, Z. Naturforsch. **37a**, 1115 (1982).
[12] P. Lamparter, W. Sperl, G. Rainer-Harbach, and S. Steeb, Z. Naturforsch. **36a**, 419 (1981).
[13] P. Lamparter, W. Sperl, E. Nold, G. Rainer-Harbach, and S. Steeb, Proc. 4th Int. Conf. Rapidly Quenched Metals, Sendai 1981, p. 343.
[14] T. E. Faber and J. M. Ziman, Phil. Mag. **11**, 153 (1965).
[15] A. Bhatia and D. E. Thornton, Phys. Rev. **B2**, 3004 (1970).
[16] Neutron Beam Facilities at the HFR available for Users, ILL, Grenoble 1981.
[17] H. H. Paalmann and C. J. Pings, J. Appl. Phys. **33**, 2635 (1962).
[18] J. Krogh Moe, Acta Cryst. **9**, 951 (1956).
[19] V. F. Sears, Adv. Phys. **24**, 1 (1975).
[20] G. E. Bacon, Neutron Diffraction, 3rd ed., Clarendon Press, Oxford 1975.
[21] L. Koester, in Neutron Physics, Springer Tracts in Modern Physics **80**, 1 (1977).
[22] G. Kostorz and S. W. Lovesey, in Treatise on Material Science and Technology 4, Vol. **15**, Academic Press, New York 1979, p. 6.
[23] G. Placzek, Phys. Rev. **86A**, 377 (1952).
[24] W. Hume Rothery and G. V. Raynor, The Structure of Metals and Alloys, 3rd ed., Inst. Metals, London 1954, p. 94.
[25] L. Pauling, The Nature of the Chemical Bond, 3rd. ed., Ithaca, Cornell Univ. Press, New York 1960, p. 246.
[26] P. Rabe and R. Haensel, in Festkörperprobleme **XX**, 43 (1980).
[27] P. Lamparter, E. Nold, G. Rainer-Harbach, E. Grallath, and S. Steeb, Z. Naturforsch. **36a**, 165 (1981).
[28] J. M. Cowley, J. Appl. Phys. **21**, 24 (1950).
[29] G. S. Cargill III and F. Spaepen, J. Non Cryst. Sol. **43**, 91 (1981).
[30] J. Blétry, Doctor-Thesis, University Grenoble 1979.
[31] J. Blétry, Z. Naturforsch. **33a**, 327 (1977).
[32] R. W. G. Wyckoff, Crystal Structures, 2nd ed., Vol. **2**, Interscience, New York 1963, p. 114.
[33] P. H. Gaskell, J. Non Cryst. Sol. **32**, 207 (1979).